Research Laboratory for the work reported in this paper. R. A. Moyle capably designed the jet impactor and several atomizer nozzles used in the aerosol generator described herein.

REFERENCES

1. J. P. Yu, E. M. Sparrow and E. R. G. Eckert, A smoke generator for use in fluid flow visualization, *Int. J. Heat Mass Transfer* **15**, 557–559 (1972).
2. G. H. Koopmann, The vortex wakes of vibrating cylinders at low Reynolds numbers, *J. Fluid Mech.* **38**, 501–512 (1967).
3. M. M. Zdravkovich, Smoke observations of the wake of a group of three cylinders at low Reynolds numbers, *J. Fluid Mech.* **32**, 339–351 (1968).
4. M. M. Zdravkovich, Smoke observations of the wakes of tandem cylinders at low Reynolds numbers, *Aero J. Royal Aero. Soc.* 108–114 (1972).
5. *Chemical and Plastics Physical Properties Tables*, pp. 10–11. Union Carbide Corporation (1969).
6. W. H. Echols and J. A. Young, Studies of portable air-operated aerosol generators, Naval Research Laboratory (NRL) Report 5929 (1963).
7. O. M. Griffin, The unsteady wake of an oscillating cylinder at low Reynolds number, *J. Appl. Mech.* **38**, 729–738 (1971).
8. O. M. Griffin, Flow near self-excited and forced vibrating circular cylinders, *J. Engng Ind.* **94**, 539–547 (1972).
9. C. W. Votaw and O. M. Griffin, Vortex shedding from smooth cylinders and stranded cables, *J. Basic Engng* **93**, 457–461 (1971).
10. J. W. Schaefer and S. W. Eskinazi, An analysis of the vortex street generated in a viscous fluid, *J. Fluid Mech.* **6**, 241–259 (1959).
11. O. M. Griffin, The effects of synchronized vibrations on vortex formation and strength, velocity fluctuations, and mean flow, *Proceedings of the IUTAM Symposium on Flow-Induced Structural Vibrations*, Karlsruhe, Germany (1972).

Int. J. Heat Mass Transfer. Vol. 16, pp. 219–223. Pergamon Press 1973. Printed in Great Britain

MELTING HEAT TRANSFER WITH WATER JET

YIN-CHAO YEN* and ANTHONY ZEHNDER

U.S. Army Cold Regions Research and Engineering Laboratory, Hanover, N.H 03755, U.S.A.

(*Received* 3 *May* 1972 *and in revised form* 3 *August* 1972)

NOMENCLATURE

- d, nozzle diameter [cm];
- D, diameter of the cavity [cm];
- g, gravitational constant [980 cm/s^2];
- h, heat transfer coefficient [cal/cm^{2}s°C];
- k, thermal conductivity of water [cal/cms°C];
- M, melting flux [g/cm^{2}s];
- Nu, Nusselt number (hd/k);
- Pr, Prandtl number $(C_p\mu/k)$;
- Re, Reynolds number $(dV\rho/\mu)$;
- s, thickness of the ice block [cm];
- T_w, water jet temperature [°C];
- T_i, ice temperature [°C];
- v, average water jet velocity [cm/s];
- V_0, nozzle water jet velocity [cm/s];
- W, melting rate [g/s];
- z, distance between nozzle tip and the initial ice surface [cm];
- λ_f, latent heat of fusion [cal/g];
- μ, viscosity of water [g/cms];
- ρ, density of water [g/cm^3];
- ρ_i, density of ice [g/cm^3].

* Also Visiting Professor of Chemical Engineering, University of New Hampshire, Durham, N.H.

INTRODUCTION

The application of high speed water jets in the mining and excavating industry is being realized as an effective and economical means for tunneling. The jets have the advantage that there are no parts in direct contact with the medium, thus preventing tool wear, and no change of equipment is necessary when going from soft to hard formations [1–3]. However, application of water jets to excavate frozen medium needs further considerations of heat-transfer characteristics of the medium. Due to the complex nature of the system, not much theoretical treatment has been given to the jet heat-transfer problem and few experimental data are available in the literature.

Some investigators [4–8] have observed two regions when the fluid jet strikes the target surface at right angles: an impingement region and a wall jet region. In the impingement region, the flow is of exceedingly complex nature and the heat-transfer coefficients are dependent upon the distance between nozzle tip and the target surface (z/d). In the wall jet region the local coefficients decrease monotonically with increasing x/d and are independent of z/d. Gardon and Akfirat [5] indicated a strong influence of D/d on the average heat transfer coefficient (D is the diameter of the target surface).

Most of the experimental work was with air jets. Friedman and Muller [9] reported their experimental data regarding average heat transfer rates of multiple jet air flow from slots, holes and nozzles parallel to or impinging on the heat transfer surface. Vickers [10] studied local heat transfer coefficients of an air jet impinging on a normal surface in the Reynolds number region 250–950 with the normal surface at $8d$–$20d$ for a nozzle diameter of 0·0507 in. Gordon and Cobonque [6] measured local as well as average heat transfer coefficients for single and multiple nozzle jets at a Reynolds number of 7000–112000 with the nozzle diameter 0·125–0·354 in. In a most recent study, Sitharamayya and Raju [11] measured the heat transfer rate between a submerged water jet and a normal plate in the Reynolds number 2000–40000 for $8 < D/d < 58$ and the average heat transfer coefficient was found to be independent of nozzle to plate distance for $z/d < 7$.

To the authors' knowledge, no one has attempted to study the problem between a fluid jet and a melting body. The present study was made on a vertical water jet striking a cylindrical ice block suspended above the nozzle. Several new problems arise by using ice as the target plate. The stagnation point is now retreating as ice melts. The melting of ice is accomplished by direct jet impingement and downward flow along the cavity. This downward flow results from the scattering of water upon impingement and on gravity. The purpose of this study is to explore the use of water jets in excavating frozen ground, and to remove ice from equipment and facilities encountered in cold regions during severe winter conditions.

EXPERIMENTAL APPARATUS AND PROCEDURE

Figure 1 shows a schematic layout of the experimental set-up. The cylindrical ice sample is 22·9 cm dia. and 22·9 cm in height. The sample container was made from a lucite tube 1·27 cm thick with an aluminum disc fastened to one end. At the center of the disc, a hook was provided to suspend the sample from the load cell. The other lucite tube which is 30·5 cm dia. and 91·4 cm in height serves a dual purpose for the experiment: to provide a support for the load cell and to contain the splashing that results from the impingement of the water jet on the ice.

An aluminum disc was also fastened to the lower end of the outer lucite tube. At the center of this disc, a sleeve was provided to hold the nozzle in a vertical position and to give an easy method of adjustment for initial nozzle-to-ice distance. A drain was also attached off to one side of the disc. A calibrated thermistor was mounted in the water supply line to the nozzle to measure water temperature during experimentation with a Fluke galvanometer.

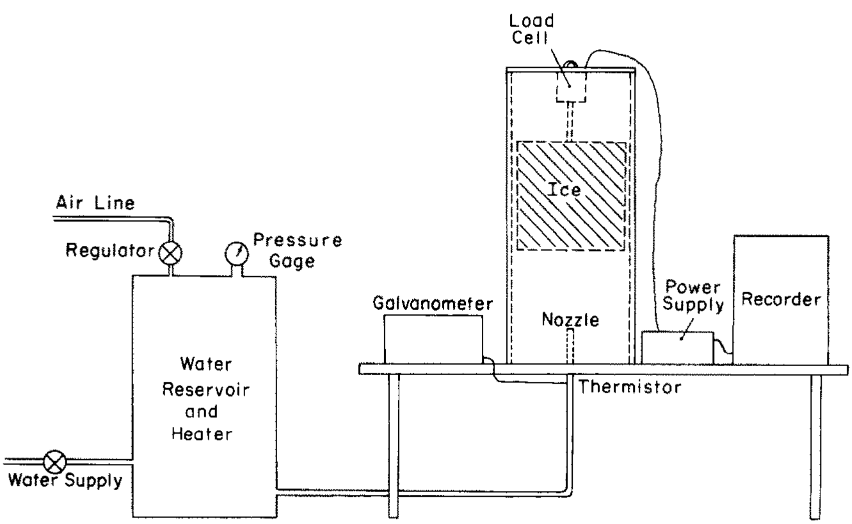

FIG. 1. Schematic of the experimental apparatus.

The load cell holds the ice sample and provides a means for measuring the weight loss of the sample. A constant power supply unit activates the load cell and the output is indicated with a Leeds and Northrop recorder.

The water supply to the nozzle was preheated to a desired temperature in a water reservoir and heater. An air line and regulator were installed at the top of the reservoir to insure a constant water pressure.

Before making an experimental run several preliminary steps are necessary. The water in the reservoir must be heated to a desired temperature and the cylinder of ice must be within the proper weight range. Since the experiment melts only 200–800 g of ice, a 0–50 lb range load cell does not provide adequate accuracy in a normal application. To circumvent this problem a tare weight system was used to calibrate the 10 in. wide strip chart recorder for a 1000 g weight loss. Adjustment of power supplied to the load cell and the millivolt input to the recorder made the procedure simple enough to check the calibration before each run. Weight of the ice sample must be controlled to insure that it is near the high side of the tare plus 1000 g or as it melts an off-scale reading results.

After calibrating and setting the nozzle tip at a desired distance from the initial ice surface, the air pressure regulator is adjusted while water is running through a rubber by-pass tube away from the ice. With the recorder in operation and a constant water temperature reading at the nozzle, removing the by-pass begins an experimental run. Duration of a run is about 15–60 s depending on the water jet parameters. The melting rate is found from the chart recorder by measuring the slope of the weight-loss curve.

A run is considered to be complete when the ice has been melted just to the top of the ice sample at the aluminum plate. This point was determined by observation of a metal washer falling from the top of the sample. The washer was simply frozen into the top of the sample by placing it in the container while the container was still inverted and the water had not yet been frozen.

Water jet flow rates were calibrated for various air pressures from 2·0 to 10·0 psi. These air pressures provided Reynolds numbers from 6000 to 40000 in the nozzle, depending upon the particular pressure and nozzle diameter. Pressures below 2·0 psi were not used because large errors could be incurred at pressure readings near zero, and at high pressures the ice melted so rapidly that the recorder readings became inaccurate.

RESULTS AND DISCUSSION

Fifty-one experiments were conducted covering a water temperature range from 17·5 to 56·0°C with a corresponding Prandtl number, Pr, variation of 7·48–3·49. Two sizes of nozzles, 0·159 and 0·238 cm dia. (d), were used along with three distances between nozzle tip and initial ice surface, 5·5, 11 and 16·5 cm corresponding to a z/d variation of 23·1–69·5. The average water velocity varied from 345·1 to 779·4 cm/s. During an experiment it was difficult to maintain the desired temperature of the water heater; therefore, water jets in essentially three temperature ranges (19·6°, 40·3° and 54·9°C) were obtained.

Observation of the ice block at the completion of a run

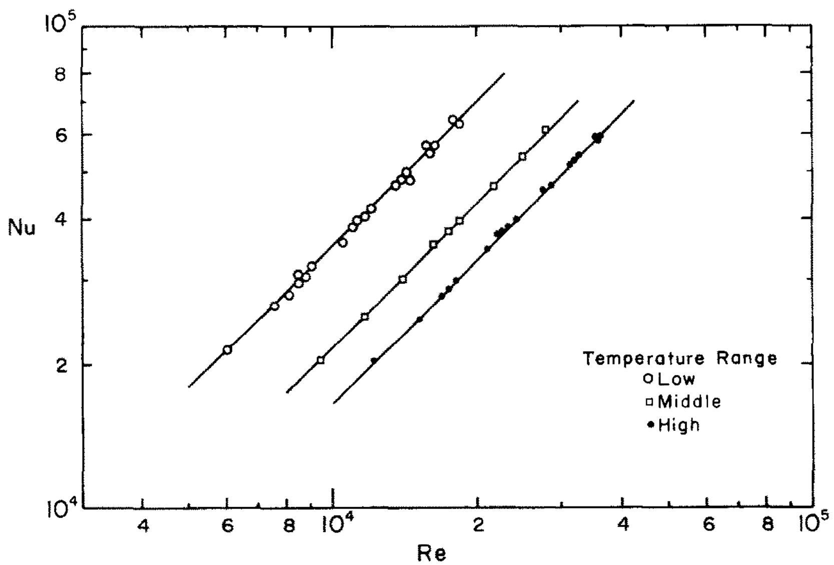

FIG. 2. Relationship between Nu and Re.

showed the walls of the hole in the ice to be essentially vertical, similar to that of a drill bit in metal with the exception that the walls were rough rather than smooth. The weight loss-time curves were found to be essentially linear, therefore the melting rate can be considered to be constant during the short duration of the experiments encountered in this investigation.

In the preliminary runs, determination of the actual amount of ice melted was accomplished by measuring the water required to fill the cylindrical cavity. A density correction factor was applied to account for phase transition. The melting rate, W, obtained in this manner closely agreed with the slope obtained from the chart recorder sheet.

The duration of the experiment, t, as indicated in the chart recorder sheets could have been used to estimate the hole size at the completion of the experiment. This can be calculated from the relation $\frac{1}{4}\pi D^2 \rho_i s = wt$ where D is the hole diameter created at the completion of the experiment and s is the ice thickness (equal to the depth of hole created). The sizes of the cavity created can be expected to be dependent on water jet temperature, velocity, nozzle diameter, duration of the experiment, initial ice temperature and initial nozzle-to-ice distance.

The chart recorder sheets were discarded without recording t. Therefore, in calculating melting flux, M, the nozzle area is used. The heat transfer coefficients are calculated from

$$h = \frac{M\lambda_f}{T_w - T_i} \quad (1)$$

where λ_f is the latent heat of fusion, T_w and T_i are the water jet and ice temperature respectively. All the physical properties μ, k, ρ were evaluated at the water jet temperature. The velocity V in the Reynolds number $dV\rho/\mu$ is calculated from

$$V = \sqrt{[V_0^2 - 2g(z + \tfrac{1}{2}s)]} \quad (2)$$

where g is the gravitational constant, V_0 is water velocity at the nozzle tip.

A plot of Nu vs. Re for the three temperature ranges produced three essentially parallel lines (Fig. 2). A crossplot of these lines indicates a Prandtl number effect to the first power, indicating a pronounced effect of temperature. The resulting plot of Nu/Pr vs. Re (Fig. 3) gives a straight line with a least squares slope of 0·94 and can be represented by

$$Nu = 0{\cdot}88\, Re^{0{\cdot}94}\, Pr \quad (3)$$

for $6000 < Re < 40000$ with a correlation coefficient of 0·983. It should be noted in Fig. 2 that the data for the various nozzle-to-ice surface distance are lumped together in each temperature range. No effect of this parameter was observed for the z/d range covered in this experiment. Furthermore, only one ice temperature was studied in this experiment (the ice sample was conditioned to near melting point in a large cold room before the experiment); however, a small change in ice temperature can be expected to have negligible effect on the correlation presented in equation (3), since the latent heat of fusion of ice is much greater than its specific heat.

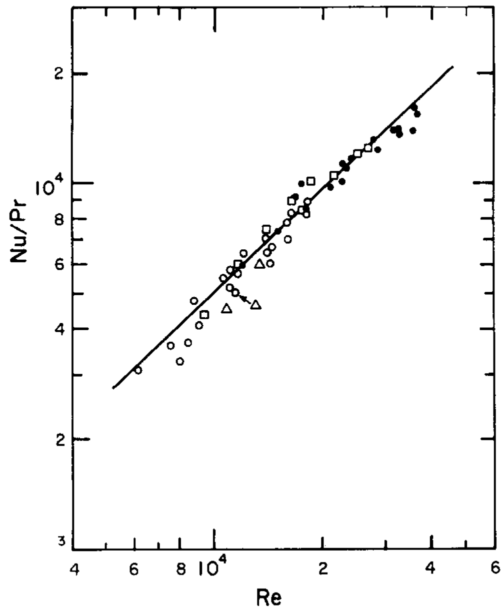

FIG. 3. Relationship between Nu/Pr and Re.

REFERENCES

1. High-speed water jets developed for use in tunneling, *Min. Congr. J.* **56**(10), 21 (1970).
2. High-speed water jets for tunneling, *Mech. Engng* **92**(11), 43 (1970).
3. Water jets are proposed as rock-cutting medium for rapid tunneling, *Engng Min. J.* **172**(1), 89 (1971).
4. M. T. SCHOLTZ and O. TRASS, Mass transfer in the laminar radial wall jet, *A.I.Ch E. Jl* **9**, 548–554 (1963).
5. R. GARDON and J. C. AKFIRAT, Heat transfer characteristics of impinging two-dimensional air jets, *J. Heat Transfer* **88C**, 101–108 (1966).
6. R. GARDON and T. COBONPUE, Heat transfer between a flat plate and jets of air impinging on it, *Int. Dev. Heat Transfer*, pp. 454–460 ASME, New York (1963).
7. V. V. RAO and O. TRASS, Mass transfer from a flat surface to an impinging turbulent jet, *Can. J. Chem. Engng* **42**, 95–99 (1964).
8 R. GARDON and J. C AKFIRAT, The role of turbulence in determining the heat transfer characteristics of impinging, *Int. J. Heat Mass Transfer* **8**, 1261–1272 (1965).

9. S. J Friedman and A. C Mueller, Heat transfer to flat surfaces, Proc. general discussion on heat transfer, Inst. Mech. Engrs., London, 138–142 (1951).
10. J. M. F. Vickers, Heat transfer coefficients between fluid jets and normal surfaces, *Ind. Engng Chem.* **51**, 967–972 (1959).
11. S. Sitharamayya and K. S. Raju, Heat transfer between an axisymmetric jet and a plate held normal to the flow, *Can. J. Chem. Engng* **47**, 365–368 (1969).